

RHEX, a novel regulator of human erythroid progenitor cell expansion and erythroblast development

Rakesh Verma,¹ Su Su,¹ Donald J. McCrann,¹ Jennifer M. Green,² Karen Leu,² Peter R. Young,² Peter J. Schatz,² Jeffrey C. Silva,³ Matthew P. Stokes,³ and Don M. Wojchowski¹

¹COBRE Center of Excellence in Stem Cell Biology and Regenerative Medicine, Maine Medical Center Research Institute, Scarborough ME, 04074

²Affymax, Inc., Palo Alto, CA 94304

³Cell Signaling Technology, Inc., Danvers, MA 01923

Ligation of erythropoietin (EPO) receptor (EPOR) JAK2 kinase complexes propagates signals within erythroid progenitor cells (EPCs) that are essential for red blood cell production. To reveal hypothesized novel EPOR/JAK2 targets, a phosphotyrosine (PY) phosphoproteomics approach was applied. Beyond known signal transduction factors, 32 new targets of EPO-modulated tyrosine phosphorylation were defined. Molecular adaptors comprised one major set including growth factor receptor-bound protein 2 (GRB2)-associated binding proteins 1–3 (GAB1–3), insulin receptor substrate 2 (IRS2), docking protein 1 (DOK1), Src homology 2 domain containing transforming protein 1 (SHC1), and sprouty homologue 1 (SPRY1) as validating targets, and SPRY2, SH2 domain containing 2A (SH2D2A), and signal transducing adaptor molecule 2 (STAM2) as novel candidate adaptors together with an ORF factor designated as regulator of human erythroid cell expansion (RHEX). *RHEX* is well conserved in *Homo sapiens* and primates but absent from mouse, rat, and lower vertebrate genomes. Among tissues and lineages, RHEX was elevated in EPCs, occurred as a plasma membrane protein, was rapidly PY-phosphorylated >20-fold upon EPO exposure, and coimmunoprecipitated with the EPOR. In UT7epo cells, knockdown of RHEX inhibited EPO-dependent growth. This was associated with extracellular signal-regulated kinase 1,2 (ERK1,2) modulation, and RHEX coupling to GRB2. In primary human EPCs, shRNA knockdown studies confirmed RHEX regulation of erythroid progenitor expansion and further revealed roles in promoting the formation of hemoglobinizing erythroblasts. RHEX therefore comprises a new EPO/EPOR target and regulator of human erythroid cell expansion that additionally acts to support late-stage erythroblast development.

CORRESPONDENCE

Don M. Wojchowski:
wojchd@mmc.org

Abbreviations used: EPC, erythroid progenitor cell; EPO, erythropoietin; EPOR, EPO receptor; ERK, extracellular signal-regulated kinase; GPA, glycophorin-A; GRB2, growth factor receptor-bound protein 2; HBB, hemoglobin-beta; LC-MS/MS, liquid chromatography-tandem mass spectrometry; NT, amino-terminal; PY, phosphotyrosine; RHEX, regulator of human erythroid cell expansion; STF, signal transduction factor; WGA, wheat germ agglutinin.

In response to hypoxia, erythropoietin (EPO) is produced by and released from renal interstitial fibroblasts (Asada et al., 2011). As predominantly expressed by erythroid progenitor cells (EPCs), EPO's cell surface receptor (EPOR) provides essential signals for pro-erythroblast and erythroblast formation (Wu et al., 1995). EPO/EPOR ligation is known to activate JAK2 kinase, JAK2 phosphorylation of EPOR cytoplasmic phosphotyrosine (PY) motifs, and canonical STAT, PI3K, and RAS/MEK/extracellular signal-regulated kinase (ERK) signal transduction pathways (Wojchowski et al., 2010; Watowich, 2011). Recently, new concepts concerning EPO-EPOR response pathways have been generated

(Broxmeyer, 2013). Transferrin receptors 1 and 2 each can modulate EPOR signaling (Forejtniková et al., 2010; Coulon et al., 2011); *Bclx* expression may not be so tightly coupled to EPOR activation and instead may have more of an effect on late-stage erythroblast formation (Rhodes et al., 2005; Singh et al., 2012a); and transcriptome-based studies have pointed to several new candidate EPO/EPOR mediators. Examples include Cyclin G2 as an EPO/EPOR/Stat5-repressed

© 2014 Verma et al. This article is distributed under the terms of an Attribution-Noncommercial-Share Alike-No Mirror Sites license for the first six months after the publication date (see <http://www.rupress.org/terms>). After six months it is available under a Creative Commons License (Attribution-Noncommercial-Share Alike 3.0 Unported license, as described at <http://creativecommons.org/licenses/by-nc-sa/3.0/>).

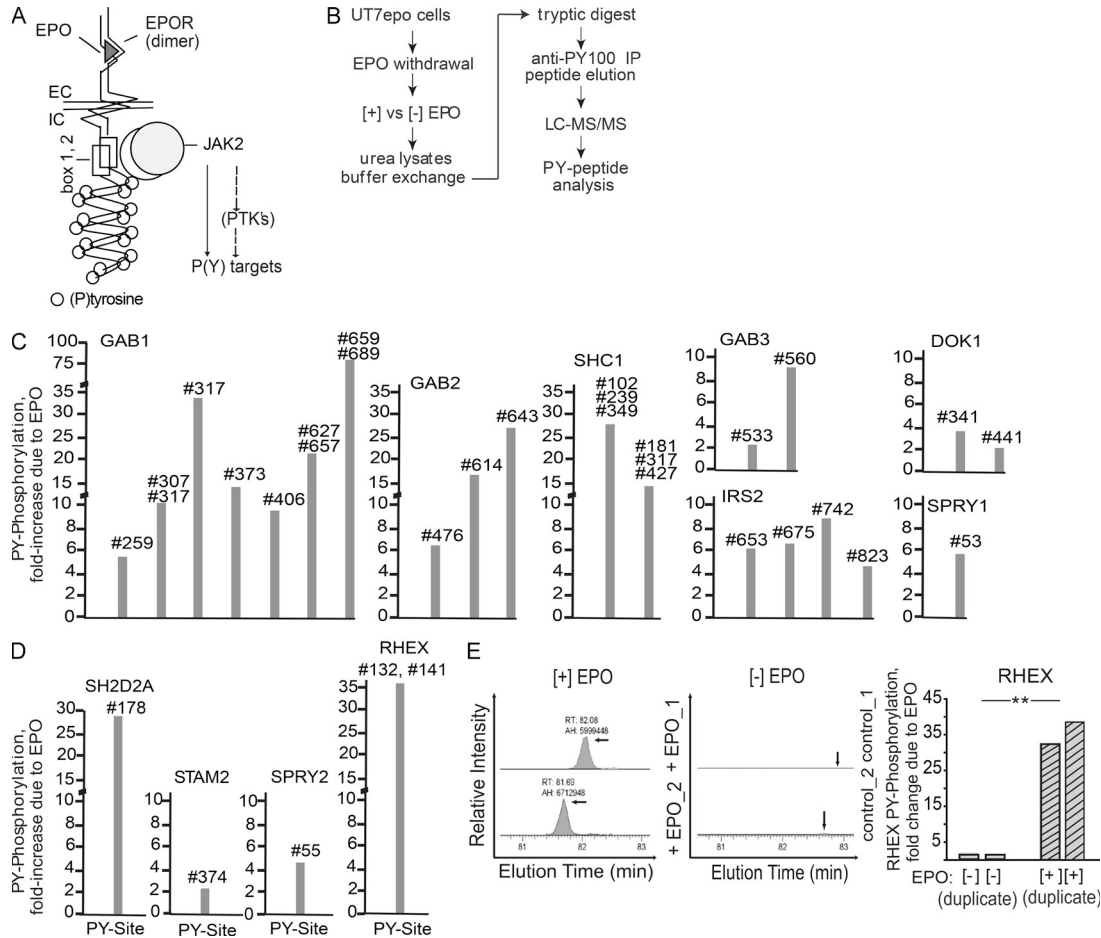


Figure 1. Phosphoproteomic analysis of EPO/EPOR PY-regulated molecular adaptors including RHEX. (A) The hEPOR is depicted, including cytoplasmic PY sites (-o-), a box1,2 JAK2 binding domain, and JAK2 plus possible protein tyrosine kinase routes to PY targets. (B) PY-phosphoproteomic steps used to define EPO/EPOR-regulated targets in UT7epo EPCs. (C and D) For a major functional subset of EPO/EPOR signal transducers as molecular adaptors, LC-MS/MS data are summarized, including fold regulation at defined PY residues. Validating targets are GAB1-3, SHC1, IRS1, DOK1, and SPRY1 (C). Novel targets are SH2D2A, STAM2, SPRY2, and C10RF186/RHEX (D). (E) For RHEX (C10RF186), duplicate LC-MS/MS data are illustrated for EPO modulation at Y132 plus Y141 sites (single tryptic peptide; and are representative of two independent analyses; **, $P \leq 0.01$, Student's t test).

regulator of cell cycle progression (Fang et al., 2007), MASL1 as a RAF-interacting inducer of EPO-dependent erythropoiesis (Kumkhaek et al., 2013), and Spi2A as an EPO-induced inhibitor of leached lysosomal executioner cathepsins (Dev et al., 2013).

To provide new insight into EPO/EPOR effects, we presently have applied a global PY-phosphoproteomics approach. One strongly regulated novel EPOR target is designated as regulator of human erythroid cell expansion (RHEX). We first characterize RHEX's genealogical representation plus stage- and lineage-restricted expression, plasma membrane localization, and EPOR co-association. In functional contexts, loss-of-function investigations then define RHEX effects on EPC growth, ERK1,2 regulation, and growth factor receptor-bound protein 2 (GRB2) association. In primary hEPCs, RHEX is further revealed to modulate the development of maturing erythroblasts. RHEX thus has evolved as an important upstream mediator of EPO/EPOR-dependent human red cell production.

RESULTS AND DISCUSSION

EPO ligation of dimeric EPOR complexes activates JAK2 kinase and the phosphorylation of nine EPOR cytoplasmic PY motifs (Fig. 1 A). Certain signal transduction factors (STFs) that dock at EPOR PY sites are well defined (e.g., p85 α at PY480, STAT5 at PY344) and some are also direct JAK2 targets (e.g., STAT5, phospholipase C γ), whereas others couple to downstream signaling modules (Wojchowski et al., 2010; Watowich, 2011; Broxmeyer, 2013). To seek novel EPOR STFs, a PY-phosphoproteomic approach was applied using UT7epo cells as a human EPC model (Komatsu et al., 1993). This involved hematopoietic growth factor withdrawal with or without EPO challenge, tryptic digests of lysates, and PY peptide isolation plus liquid chromatography-tandem mass spectrometry (LC-MS/MS) identification (Fig. 1 B). Overall, 54 unique EPO/EPOR-modulated PY proteins were identified with ≥ 2.5 -82.6-fold modulation (Table S1). These included known STFs modulated at known PY sites, known

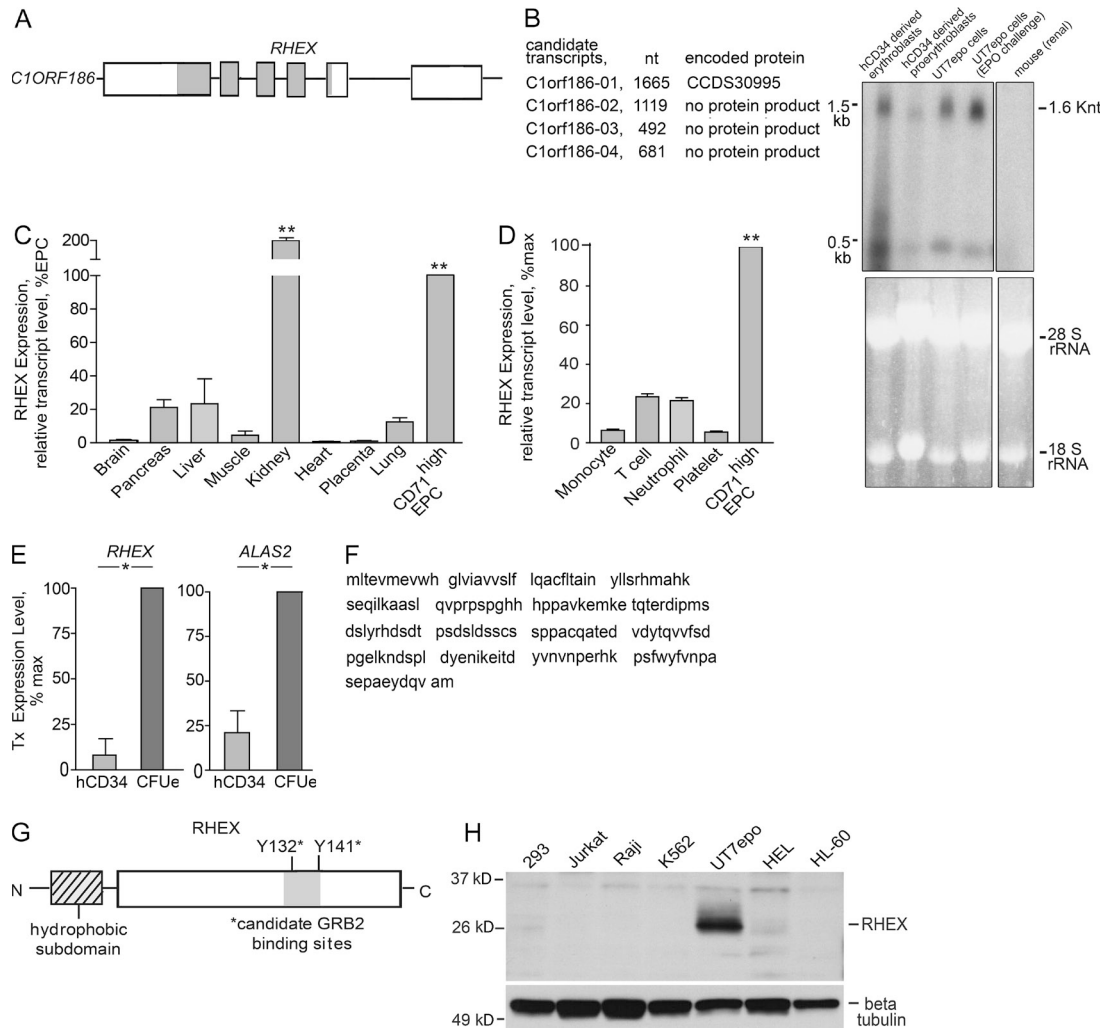


Figure 2. RHEX locus, transcripts, and primary protein structure. (A) *C1ORF186/RHEX* gene structure. (B) Analyses of putative *RHEX* transcripts (top) and Northern blotting (bottom) defined major 1.6 kb nt (and minor <0.5 kb nt) transcripts in UT7epo cells, and in primary human EPCs. (C and D) RT-PCR assays of *RHEX* transcript expression levels in primary human tissues (C) and among human peripheral blood monocytes, T cells, neutrophils, and platelets (as compared with primary CD71^{high} EPCs; D). (For elevated *RHEX* levels in EPCs and kidney, $P \leq 0.01$; **, Student's *t* test, representative of two independent analyses). (E) RNA-Seq analyses of *RHEX* (and *ALAS2*) transcript levels in primary human CD34^{pos} progenitors and CFUe. (*, $P \leq 0.05$, Student's *t* test, single experiment). (F and G) Primary sequence of RHEX (F) and candidate functional domains (G). (H) Western blot analysis of RHEX protein expression among human hematopoietic cell lines (representative of two independent studies).

STFs modulated at novel sites, known proteins not previously associated with EPO/EPOR signaling, and novel targets encoded by predicted ORFs. As one major functional subset, 11 targets proved to be molecular adaptors. GAB1-3, SHC1, IRS2, DOK1, and SPRY1 comprise known (and validating) targets (Fig. 1 C), whereas SH2D2A, STAM2, and SPRY2, together with a *C1ORF186* product, represent novel candidate EPO/EPOR STFs (Fig. 1 D). *C1ORF186* (designated as RHEX) was up-modulated by EPO ≥ 20 -fold in its phosphorylation at PY132 and PY141 sites (single PY peptide; Fig. 1 E) and is this report's prime focus.

RHEX is encoded at a six-exon *C1ORF186* locus (Fig. 2 A) that generates a singular predicted 1.6 kb nt coding transcript. Northern blotting detected major 1.6 kb, and minor <0.5 kb nt

transcripts (Fig. 2 B). Interestingly, *RHEX* proved to be well conserved in *Homo sapiens* and primates (99% nt conservation) but was not detected in rat, mouse, or lower vertebrate genomes. *RHEX* transcript expression among tissues and blood cells was also investigated and was relatively high level in primary human EPCs and kidney (Fig. 2, C and D). RNA-Seq also indicated elevated *RHEX* levels in CFUe as compared with CD34^{pos} progenitors (Fig. 2 E). At a protein level, RHEX's predicted domains included an amino-terminal (NT) hydrophobic region and two carboxy-terminal candidate GRB2 binding sites (Neumann et al., 2009; Fig. 2, F and G). RHEX, however, is unique and exhibits homology only with limited residues of a recently reported erythrocytic spectrin (NP_003117.2). Basic assessments of RHEX levels among

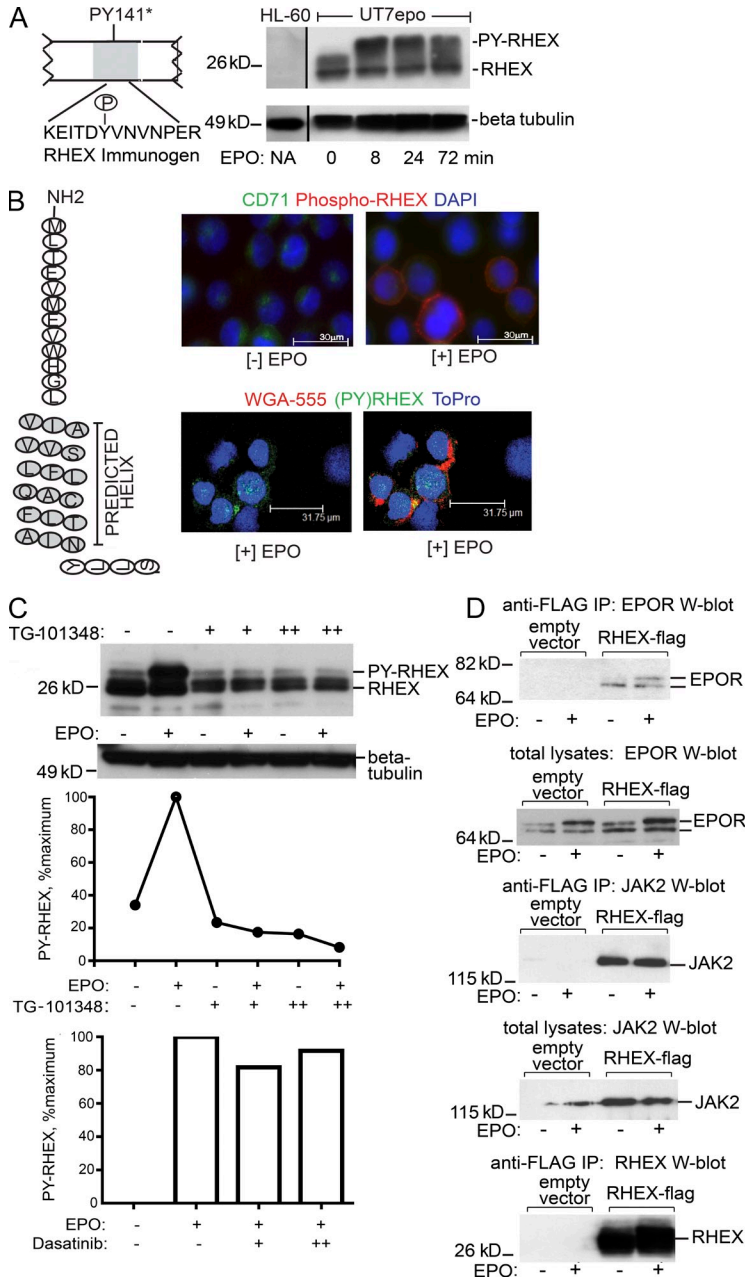


Figure 3. RHEX regulation by EPO, plasma membrane localization, JAK2 phosphorylation, and RHEX/EPOR/JAK2 coimmunoprecipitation. (A) A rabbit mAb to (PY)RHEX was prepared and used in Western blot analyses of EPO-challenged UT7epo cells to validate EPO-induced RHEX PY phosphorylation (representative of three independent analyses). Black lines indicate that intervening lanes have been spliced out. (B) After cytokine withdrawal, UT7epo cells were challenged with EPO (± 3 U/ml). At 15 min, cells were cytospun, fixed, and assayed by confocal immunofluorescence microscopy for PY-RHEX localization (right). In top paired panels (– vs. + EPO), CD71 was co-stained (right). In lower paired panels (+ EPO), cells were co-stained with AF555-WGA (representative of two independent experiments). RHEX’s predicted N-terminal α -helical transmembrane domain is also diagrammed. (C) UT7epo cells were exposed to TG101348 (0, 5, and 15 nM, indexed as –, +, and ++). After HGF withdrawal, cells were exposed to 2 U/ml EPO. At 10 min, lysates were prepared and analyzed for levels of (PY)RHEX. Effects of SRC inhibition by Dasatinib on EPO-induced PY-RHEX formation also were assessed (+ and ++ as 50 and 150 nM; bottom). Results are representative of two independent experiments. (D) UT7epo cells were stably transduced with lentivirus encoding a Flag epitope-tagged RHEX (carboxy-terminal tag). In anti-Flag immunoprecipitations, the EPOR (top pair of panels) and JAK2 (center pair of panels) were observed to co-immunoprecipitate with RHEX-(Flag) (representative of two independent experiments). In the bottom panel, the immunoprecipitation of RHEX-(Flag) on its own is shown.

human hematopoietic cell lines (and 293 cells) using polyclonal antiserum to RHEX further revealed expression only in erythroid UT7epo cells (Fig. 2 H).

To analyze RHEX’s subcellular localization and actions, a (PY)RHEX reactive monoclonal antibody was next generated and was used in UT7epo cells to first validate rapid EPO induction of PY-RHEX (Fig. 3 A and not depicted). Human SCF, IL3, GM-CSF, TPO, Flt3L, or serum, in contrast, did not detectably stimulate RHEX’s PY phosphorylation (unpublished data). RHEX’s hydrophobic NT region prompted subcellular localization analyses. As indicated by CD71 and wheat germ agglutinin (WGA) markers, (PY)RHEX resided at the plasma membrane (Fig. 3 B). Experiments using JAK2 and SRC kinase

inhibitors (TG101348 and Dasatinib, respectively) pointed to RHEX as a JAK2 target (Fig. 3 C). Beyond this, coimmunoprecipitation experiments using an RHEX-flag construct indicated co-association with EPOR and JAK2 complexes (Fig. 3 D).

To assess function, RHEX knockdown experiments were performed. Three assessed shRNAs each efficiently inhibited RHEX expression (Fig. 4 A and not depicted). As assayed via clonal colony formation, RHEX knockdown limited UT7epo cell growth ≥ 3 -fold (Fig. 4 B, top). Analyses in liquid culture confirmed effects on growth (with no significant effects on survival), and a parallel attenuation of ERK1,2 activity was also observed (Fig. 4, B and C). Possible effects of RHEX on murine EPCs were also studied via lentiviral expression in

G1E-ER4 cells (Welch et al., 2004). In this proerythroblast model, mEPOR ligation did not effectively induce PY-RHEX formation (Fig. 4 D). RHEX, furthermore, was unstable and no

reproducible effects on proliferation or on Gata1-ER-induced late-stage differentiation were observed (unpublished data).

RHEX's actions were next studied in human CD34^{pos} progenitor-derived EPCs. Endogenous *RHEX* transcript levels became elevated at days 5–7 of culture (pro- to basophilic erythroblasts; Fig. 5, A and B). In developmentally staged EPCs as isolated via FACS, RHEX was elevated in proerythroblasts (Fig. 5 C and not depicted). In shRNA lentivirus transduction experiments, when RHEX was knocked down, EPC expansion was attenuated (without significant effects on viability; Fig. 5, D and E). Beyond this, glycophorin-A (GPA) levels were skewed and increased when RHEX expression was inhibited (Fig. 5 F). Cytospin morphologies also revealed apparent effects of RHEX knockdown on erythroid development, including a delayed formation of maturing normoblasts (Fig. 5 G). By inspection of cell pellets, Western blotting, and RT-PCR, hemoglobinization was also attenuated, which is further consistent with a role for RHEX in supporting erythroblast development at a normoblast stage (Fig. 5, H and I). Tests of GRB2 as a candidate RHEX partner were also advanced. As analyzed in UT7epo cells, RHEX-Flag and GRB2 coimmunoprecipitated (Fig. 5 J; as did these endogenous STFs, Fig. 5 K). Here, EPO exposure moderately increased levels of GRB2 plus RHEX coimmunoprecipitation.

Recent discoveries of novel EPOR pathways (Broxmeyer, 2013) and new EPOR agonists (Drüeke, 2013) have heightened interest in transducers of EPO's effects. Our PY-phosphoproteomic analyses first reveal several novel candidate EPOR targets as molecular adaptors, S/T kinases, tyrosine phosphatases, ubiquitin factors, and cell cycle regulators (Supplemental Table S1). A focus on RHEX was prompted by its sharp EPO modulation, ORF novelty, conserved representation in *H. sapiens* and primates, and stage-specific up-modulation in developing erythroid cells. RHEX proved to be plasma membrane-associated, to coimmunoprecipitate with the EPOR, and to comprise a likely JAK2 PY target. EPO-regulated sites Y132 and/or Y141 were also implicated to bind GRB2. Via SOS plus RAS, GRB2 may mediate RHEX effects on ERK1/2 activity, but GRB2 itself is a versatile adaptor protein that can also couple to SHIP, SHP2, and up to 90 interacting proteins (Bisson et al., 2011). GRB2 can also preassemble with RTKs and repress basal signaling (Lin et al., 2012). Merit therefore exists for future investigations of implicated RHEX PY132, PY141, and GRB2 engaged pathways.

In primary EPCs, loss of function studies confirmed RHEX effects on proliferation but also indicated additional roles during normoblast development in that RHEX knockdown led to persistent erythroblastic features, high-level GPA expression, and decreased *HBB* transcript plus globin expression. Although this might relate indirectly to observed effects of RHEX on growth, effectors that reinforce EPC growth (e.g., via RAS; Zhang and Lodish, 2007; Blanc et al., 2012) often attenuate erythroid differentiation. Apparent effects of RHEX on normoblast development, therefore, may involve alternative mechanisms (and may point to novel EPO/EPOR effects on erythroid differentiation). RHEX-regulated routes that

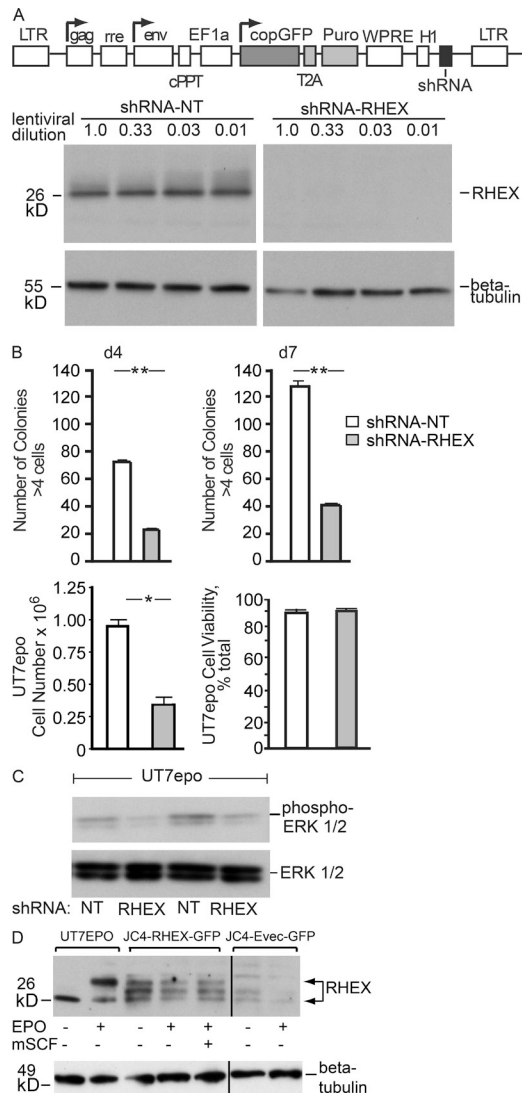


Figure 4. RHEX modulation of EPC cell growth. (A) A modified pGreenPuro lentivirus (top) was used to stably express shRNAs. Efficient knockdown of RHEX in UT7epo cells transduced at varied MOIs is illustrated (Western blot, representative of three independent experiments). (B) UT7epo cell colony formation at days 4 and 7 after transduction with shRNA-NT or shRNA-RHEX lentiviruses is summarized (mean number of >4⁺-cell colonies \pm SE, $n = 2$; **, $P \leq 0.01$, Student's *t* test, representative of two independent experiments). RHEX knockdown effects on UT7epo cell growth (and survival) are also shown for liquid culture experiments (bottom panels; day 4, mean values \pm SE, $n = 2$; *, $P \leq 0.05$, Student's *t* test, representative of two independent experiments). (C) After lentiviral transduction and culture in EPO (3 U/ml), levels of phospho-ERK1,2 were determined for UT7epo cells stably transduced with shRNA-NT or shRNA-RHEX lentiviruses (representative of two independent experiments). (D) RHEX also was stably expressed in murine G1E-ER4 proerythroblastic cells. Mouse EpoR ligation did not effectively induce PY-RHEX formation (representative of three independent experiments). Black lines indicate that intervening lanes have been spliced out.

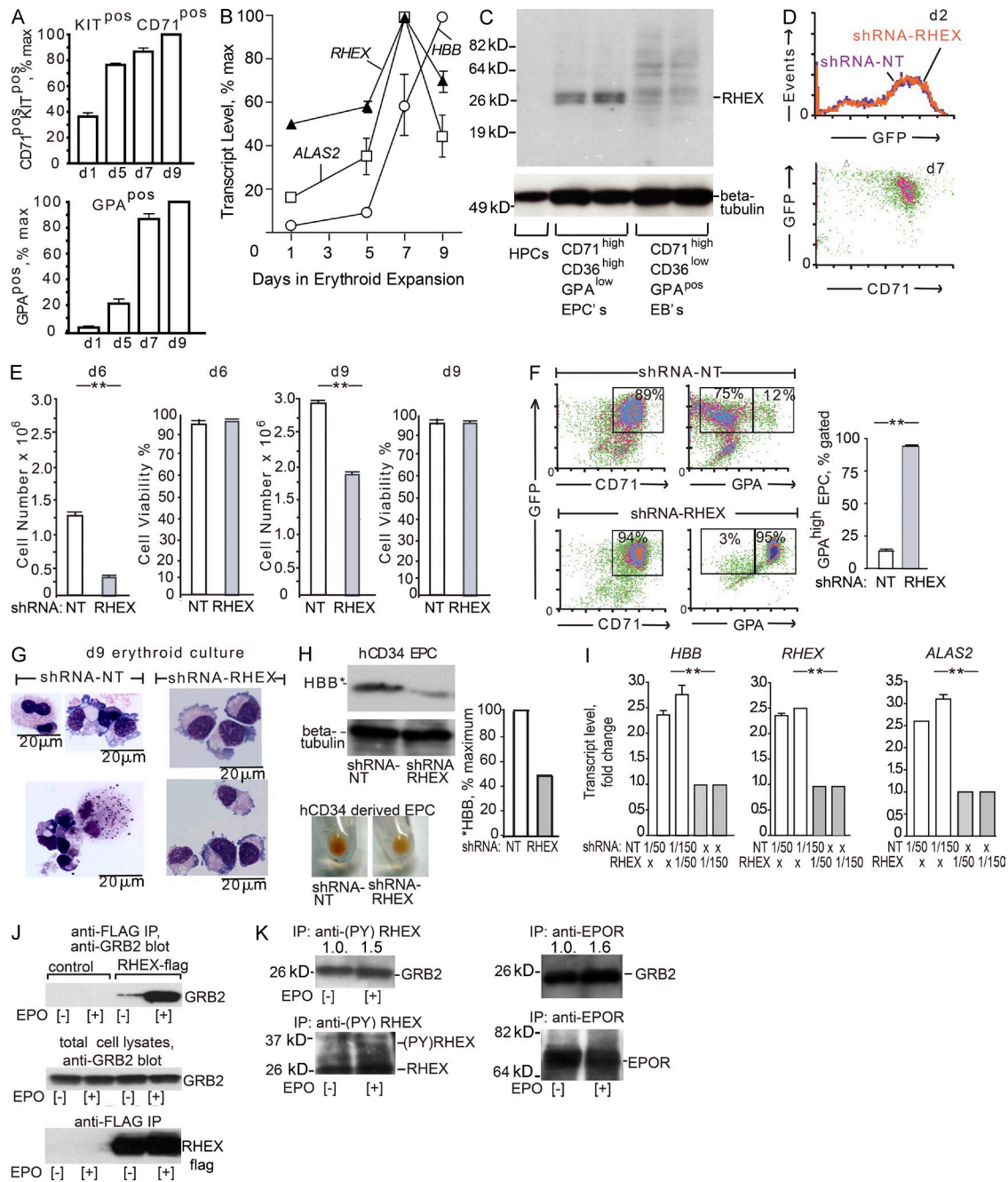


Figure 5. In primary human EPCs, shRNA knockdown reveals positive roles for RHEX during erythroid progenitor expansion and erythroblast maturation. (A) Upon a shift of CD34^{pos} progenitors to erythroid culture conditions, courses of CD71 and GPA marker expression were defined via flow cytometry. Data are normalized means \pm SE, $n = 3$ (representative of 5 independent experiments). (B) RT-PCR analyses of *RHEX* expression during EPC development ex vivo (*ALAS2*, *Aminolevulinic Acid Synthetase-2*; *HBB*, *Hemoglobin- β* ; means \pm SE, $n = 2$). (C) HPC's expanded short-term (48 h) proerythroblasts (as CD71^{high}CD36^{high}GPA^{low} EPCs) and erythroblasts (as CD71^{high}CD36^{low}GPA^{pos} EBs) were isolated (FACS) and analyzed via Western blotting for RHEX expression levels. (D) Efficient transduction of hCD34 progenitors and persistent GFP marker expression among developing CD71^{high} EPCs as demonstrated by co-positive day 7 CD71^{high}GFP^{pos} EPCs (flow cytometry analysis). (E) Decreased EPC growth (at days 6 and 9) due to RHEX knockdown (mean cell numbers \pm SE, $n = 2$; **, $P < 0.01$, Student's *t* test, representative of two independent experiments). (F) Representative expression profiles of CD71 and GPA marker expression are shown for shRNA-NT and shRNA-RHEX transduced EPCs (day 9 after transduction), together with summary data (means \pm SE, $n = 2$; **, $P \leq 0.01$, Student's *t* test, representative of two independent experiments). (G) Representative EPC morphologies are shown after shRNA-NT and shRNA-RHEX transduction (day 9). (H) Western blot analysis and visualization of hemoglobin levels in developing EPCs after transduction with shRNA-NT or shRNA-RHEX. (I) RT-PCR analyses of *HBB*, *RHEX*, and *ALAS2* (means \pm SE, $n = 2$; **, $P \leq 0.01$, Student's *t* test). (J) In UT7epo cells, coimmunoprecipitation assays demonstrated the association of RHEX-Flag with endogenous GRB2. (K) Co-immunoprecipitation of endogenous GRB2 with RHEX was also observed.

support erythroblast development, therefore, should also be of significant interest to define during myeloproliferative disease (Barbui et al., 2013) and the ineffective erythropoiesis of thalassemia (Rivella, 2012).

MATERIALS AND METHODS

Cell lines and primary hematopoietic cells. UT7epo EPC (Komatsu et al., 1993), 293, JURKAT, RAJI, K562, HL60, and HEL cell lines were maintained as previously described (Singh et al., 2012b). In cytokine withdrawal experiments, UT7epo cells were washed three times and cultured for 20 h in 0.2% BSA, 10 μ g/ml holo-transferrin, 0.1 mM 2-mercaptoethanol, and IMDM (Singh et al., 2012b). Subsequent EPO (and cytokine) challenges were at the concentrations and time intervals indicated. Primary human hematopoietic cells used in RT-PCR analyses included monocytes, neutrophils, T cells, and platelets (AllCells). Murine G1E-ER4 cells (M. Weiss, Children's Hospital of Philadelphia, Philadelphia, PA) were maintained in EPO plus mSCF as per Welch et al. (2004).

Primary EPCs were generated ex vivo from GCSF mobilized human CD34^{pos} cells. CD34^{pos} progenitors were cultured for 48 h in X-vivo10 media (Lonza) supplemented with 50 ng/ml each of rhSCF, rhIL3, rhFLT3, and rhTPO (PeproTech). For erythroid cell development, expanded progenitors were plated (at 10⁶ cells/ml) in StemSpan medium (STEMCELL Technologies) supplemented with 100 ng/ml rhSCF, 2 U/ml EPO, 100 μ g/ml holo-transferrin, 1.5 μ M β -estradiol, 0.5 μ M dexamethasone, and 0.1 mM β -mercaptoethanol. On days 2, 6, and 10, cultures received 0.6 volume of medium. On days 4, 8, and 12, cultures were replated in fresh medium (10⁶ cells/ml). Erythroid development was assessed via flow cytometry, cytospin, and RT-PCR analyses.

Phosphoproteomics and in silico analyses. In UT7epo cell PY-phosphoproteomic studies, cytokines were withdrawn for 20 h. Cells were then exposed to EPO (\pm 4 U/ml for 15 min), and 9 M urea lysates were prepared and used to generate tryptic digests (Sathyanarayana et al., 2012). For duplicate samples, PY-phosphoproteomic LC-MS/MS analyses were then applied using a PhosphoScan approach (Stokes et al., 2012). Gene and transcript analyses used NCBI programs Gene, BLAST, Homologene, Gene Expression Omnibus, and Ensembl Genome browser. RHEX's candidate structural features were assessed using BLAST Conserved Domain plus Cobalt (NCBI), ProSite (Expasy), TMHMM Server (v 2.0), and Tmpmed (chEMBL Net).

RT-PCR and Northern blotting. For RT-PCR analyses, EPCs (including FACS or MACS isolated subpopulations) were lysed in TRIZOL reagent (Invitrogen), and RNA was prepared (RNeasy; QIAGEN). Reverse transcription (Superscriptase III; Invitrogen) and real-time quantitative polymerase chain reactions (iQ SYBR Green, i-Cycler; Bio-Rad Laboratories) were performed as previously described (Dev et al., 2013). The following primer pairs were from Invitrogen: *hRHEX/C1ORF186*, *hALAS2*, *hHBB*, and *hBETA-ACTIN*. Northern blotting was performed as detailed by Pircher et al. (2001) using a randomly primed full-length ³²P-RHEX cDNA probe.

Antibodies and Western blot analyses. Rabbit antibodies to RHEX were generated by immunizations with KLH-coupled peptides and immunogen boosts. Responses were evaluated by ELISA (phosphorylated and non-phosphorylated peptides) and by Western blotting (UT7epo and HL60 cell lysates). Additional antibodies were to (P)ERK1,2, GRB2, β -TUBULIN (Cell Signaling Technology), Hemoglobin (Santa Cruz Biotechnology, Inc.), and the EPOR (Singh et al., 2012b). Western blotting was as described previously (Singh et al., 2012b). In chemiluminescence, HRP-conjugated antibodies (Jackson ImmunoResearch Laboratories, Inc.) and Super-Signal West-Dura reagent were used. In immunoprecipitations, 0.4% Igepal lysates were prepared as per Singh et al. (2012b). Antibodies used (4 μ g per immunoprecipitation) were to a RHEX-Flag epitope (Sigma-Aldrich) and the EPOR (Singh et al., 2012b). Immune complexes were retrieved using protein A/G particles (Thermo Fisher Scientific). In analyses of RHEX PY phosphorylation, cell lysates were exposed to Lambda phosphatase before SDS denaturation and

Western blotting. In JAK2 and SRC inhibitor studies, UT7epo cells were cultured for 20 h with TG101348 or Dasatinib at the indicated concentrations (0.5% DMSO, solvent).

Immunofluorescence microscopy. UT7epo cells were stained with FITC-anti-CD71, collected onto poly-L-lysine slides, exposed to 4% formaldehyde in PBS (20 min, 23°C), and then to 90% methanol (10 min, -20°C). Anti-(PY)RHEX antibody was used at 4 μ g/ml (4°C, 60 min) and was detected using an Alexa Fluor 647 anti-rabbit second antibody. Alternatively, surface staining was with 5 μ g/ml AF555-WGA for 10 min at 37°C (Life Technologies). Nuclear staining was with 1 μ M ToPro-3 iodide for 20 min (Invitrogen). Preparations were washed three times in PBS and coverslipped (1.5 mm, Corning) in VECTASHIELD (Vector Laboratories). Images were acquired and analyzed using a confocal microscope system (SP1; Leica; Dev et al., 2013).

Lentiviruses, and transductions. shRNAs (as designed with SBI) were cloned to a pGreenPuro vector modified to include an EF1 α promoter for GFP plus puromycin resistance cDNA expression. shRNA sequences were as follows: shRNA-RHEX-UTR-#1, 5'-GATCCGGAAGAAGCTTTCAGG-TAAACTTCCTGTCAGCCTTCTTGAAAGTCCATTTTTTTTGAATT-3'; shRNA-RHEX-UTR-#2, 5'-GATCCGGAGGTAAAGTATGAGAAGT-ACTTCCTGTCAGTCCATTTTCATCCTTTGATTTTTTGAATT-3'; shRNA-RHEX-UTR-#3, 5'-GATCCGGAGGAAGAAGTTCAGGTA-ACTTCCTGTCAGTCCCTTCTTGAAAGTCCATTTTTTTTGAATT-3'; shRNA-NT, 5'-GATCCCTAAGGTTAAGTCGCCCTCGCTCTAGCGA-GGGCGACTTAACCTTAGGTTTTTGAATT-3'. Packaged lentiviruses (prepared using SBI-NT 293 cells) were recovered at 50 h after transduction, 0.4 μ m filtered, concentrated (PEG-IT reagent, SBI), titered, aliquoted, and stored at -80°C. UT7epo and G1E-ER4 cell transductions involved plating cells at 3 \times 10⁵ cells/ml, and at 20 h replating to 12-well plates at 2 \times 10⁵ cells/ml (0.4 ml/well). At 4 h of culture, 4 μ g/ml polybrene was added, followed by 40 μ l shRNA-encoding lentivirus in IMDM (at defined MOIs). At 20 h after transduction, 0.5 ml of culture medium was added. At 40 h after transduction, 0.5 ml of cells were selected in 2.5 μ g/ml puromycin or plated in methylcellulose for colony forming assays (see below).

In the lentiviral knockdown of RHEX in primary human EPCs, pre-expanded cells were transduced with pGreenPuro lentiviruses encoding RHEX-targeting or nontargeting (NT) shRNAs. Specifically, nontreated 12-well tissue culture plates (BD), were coated with 20 μ g/ml Retronectin (Takara Bio Inc.), washed, and used to preadsorb lentiviruses at 37°C for 1.5 h. This was followed by centrifugation at 800 g for 25 min at 4°C. Pre-expanded hCD34^{pos} cells were plated at 0.5 \times 10⁶ cells/ml in Xvivo 10 medium (as described above) and were transduced using 3 μ g/ml polybrene (30 min incubation at 37°C) and spinoculation for 30 min at 400 g at 25°C. After culture for 20 h, transduced cells were then plated in StemSpan medium (STEMCELL Technologies) supplemented with 100 ng/ml rhSCF, 100 μ g/ml holo-transferrin, 2 U/ml EPO, 1.5 μ M β -estradiol, 0.5 μ M dexamethasone, and 0.1 mM β -mercaptoethanol. Puromycin was included at 2.5 μ g/ml. At the indicated time points, erythroid cell formation was assayed via flow cytometry (c-KIT, TFR1, GPA), cytospin morphologies, and RT-PCR. Viable cell counts (ViCell system; Beckman Coulter) and YOPRO3 viability analyses (Molecular Probes) were also performed. Lentiviral expression vectors also were prepared including those expressing RHEX-Flag (EF1 α) plus puromycin resistance cDNAs (PGK), and RHEX plus GFP cDNAs. Each template, together with empty vector negative control templates, was packaged as above and was titered using NIH3T3 cells.

Flow cytometry, colony-forming assays, and cytospin histomorphologies. Flow cytometry analyses of erythroid development used APC-anti-CD117, FITC-anti-CD71, and PE-anti-CD235a antibodies (BD), a FACSCalibur cytometer (BD), and CellQuest Pro software. In colony-forming unit assays, 0.5 \times 10⁴ transduced UT7epo cells were plated in MethoCult H4434 medium (STEMCELL Technologies) supplemented with 3 U/ml EPO and 4.0 μ g/ml puromycin. Colonies were analyzed using a STEMvision system (STEMCELL Technologies), differential interference fluorescence microscopy (DMI6000 B;

Leica), and EVOS fluorescence microscopy. Cytospin analyses (10^5 cells) involved poly-L-lysine slide centrifugation for 15 min at 100 g (Hettich Universal-16A cyto-centrifuge) and May-Grunwald Giemsa staining (Dev et al., 2013).

Online supplemental material. Table S1 shows EPO/EPOR PY-regulated targets as interrogated in UT7epo cells via PhosphoScan LC-MS/MS PY-proteomics. Online supplemental material is available at <http://www.jem.org/cgi/content/full/jem.20130624/DC1>.

Phosphoproteomic studies were advanced collaboratively via PhosphoScan LC-MS/MS with Cell Signaling Technology, Inc. Expert technical contributions of research staff (D.M. Wojchowski laboratory) are also gratefully acknowledged for human CD34 cell culture (R. Asch), RHEX antibody characterization (A. Pradeep), lentivirus construction (A. Johnson), and hEPC CD marker analyses plus FACS (E. Jachimowicz and N. Rainville). For RNA-Seq analyses of *RHEX* and *ALAS2* in CD34^{pos} progenitors and CFUE, the authors thank Drs. M. Narla and X. An (New York Blood Center), as well as Dr. M. Weiss (Children's Hospital of Philadelphia) for the generous provision of G1E-ER4 cells.

Primary support was provided by NIH R01-HL44491 (D.M. Wojchowski), with additional partial support via NIH R01 DK89439 (D.M. Wojchowski). Core facility contributions (flow cytometry, quantitative RT-PCR via Progenitor Cell Analysis and Molecular Phenotyping Cores) were supported in part via NIH/NIGMS P30GM106391 (D.M. Wojchowski). Confocal microscopy was supported in part by the Cell Imaging Core facility of COBRE Center Award P30GM103392. Supporting contributions by Affymx, Inc. and Takeda Global Research and Development Center, Inc. (Deerfield, IL) also are gratefully acknowledged.

The authors declare no competing financial interests.

Submitted: 26 March 2013

Accepted: 16 July 2014

REFERENCES

- Asada, N., M. Takase, J. Nakamura, A. Oguchi, M. Asada, N. Suzuki, K. Yamamura, N. Nagoshi, S. Shibata, T.N. Rao, et al. 2011. Dysfunction of fibroblasts of extrarenal origin underlies renal fibrosis and renal anemia in mice. *J. Clin. Invest.* 121:3981–3990. <http://dx.doi.org/10.1172/JCI57301>
- Barbui, T., G. Finazzi, and A. Falanga. 2013. Myeloproliferative neoplasms and thrombosis. *Blood.* 122:2176–2184. <http://dx.doi.org/10.1182/blood-2013-03-460154>
- Bisson, N., D.A. James, G. Ivosev, S.A. Tate, R. Bonner, L. Taylor, and T. Pawson. 2011. Selected reaction monitoring mass spectrometry reveals the dynamics of signaling through the GRB2 adaptor. *Nat. Biotechnol.* 29:653–658. <http://dx.doi.org/10.1038/nbt.1905>
- Blanc, L., S.L. Ciciotte, B. Gwynn, G.J. Hildick-Smith, E.L. Pierce, K.A. Soltis, J.D. Cooney, B.H. Paw, and L.L. Peters. 2012. Critical function for the Ras-GTPase activating protein RASA3 in vertebrate erythropoiesis and megakaryopoiesis. *Proc. Natl. Acad. Sci. USA.* 109:12099–12104. <http://dx.doi.org/10.1073/pnas.1204948109>
- Broxmeyer, H.E. 2013. Erythropoietin: multiple targets, actions, and modifying influences for biological and clinical consideration. *J. Exp. Med.* 210:205–208. <http://dx.doi.org/10.1084/jem.20122760>
- Coulon, S., M. Dussiot, D. Grapton, T.T. Maciel, P.H. Wang, C. Callens, M.K. Tiwari, S. Agarwal, A. Fricot, J. Vandekerckhove, et al. 2011. Polymeric IgA1 controls erythroblast proliferation and accelerates erythropoiesis recovery in anemia. *Nat. Med.* 17:1456–1465. <http://dx.doi.org/10.1038/nm.2462>
- Dev, A., S.M. Byrne, R. Verma, P.G. Ashton-Rickardt, and D.M. Wojchowski. 2013. Erythropoietin-directed erythropoiesis depends on serpin inhibition of erythroblast lysosomal cathepsins. *J. Exp. Med.* 210:225–232. <http://dx.doi.org/10.1084/jem.20121762>
- Drüeke, T.B. 2013. Anemia treatment in patients with chronic kidney disease. *N. Engl. J. Med.* 368:387–389. <http://dx.doi.org/10.1056/NEJMe1215043>
- Fang, J., M. Menon, W. Kapelle, O. Bogacheva, O. Bogachev, E. Houde, S. Browne, P. Sathyanarayana, and D.M. Wojchowski. 2007. EPO modulation of cell-cycle regulatory genes, and cell division, in primary bone marrow erythroblasts. *Blood.* 110:2361–2370. <http://dx.doi.org/10.1182/blood-2006-12-063503>
- Forejtniková, H., M. Vieillevoys, Y. Zermati, M. Lambert, R.M. Pellegrino, S. Guihard, M. Gaudry, C. Camaschella, C. Lacombe, A. Roetto, et al. 2010. Transferrin receptor 2 is a component of the erythropoietin receptor complex and is required for efficient erythropoiesis. *Blood.* 116:5357–5367. <http://dx.doi.org/10.1182/blood-2010-04-281360>
- Komatsu, N., M. Yamamoto, H. Fujita, A. Miwa, K. Hatake, T. Endo, H. Okano, T. Katsube, Y. Fukumaki, S. Sassa, et al. 1993. Establishment and characterization of an erythropoietin-dependent subline, UT-7/Epo, derived from human leukemia cell line, UT-7. *Blood.* 82:456–464.
- Kumkhaek, C., W. Aerbajinai, W. Liu, J. Zhu, N. Uchida, R. Kurlander, M.M. Hsieh, J.F. Tisdale, and G.P. Rodgers. 2013. MASL1 induces erythroid differentiation in human erythropoietin-dependent CD34⁺ cells through the Raf/MEK/ERK pathway. *Blood.* 121:3216–3227. <http://dx.doi.org/10.1182/blood-2011-10-385252>
- Lin, C.C., F.A. Melo, R. Ghosh, K.M. Suen, L.J. Stagg, J. Kirkpatrick, S.T. Arold, Z. Ahmed, and J.E. Ladbury. 2012. Inhibition of basal FGF receptor signaling by dimeric Grb2. *Cell.* 149:1514–1524. <http://dx.doi.org/10.1016/j.cell.2012.04.033>
- Neumann, K., T. Oellerich, H. Urlaub, and J. Wienands. 2009. The B-lymphoid Grb2 interaction code. *Immunol. Rev.* 232:135–149. <http://dx.doi.org/10.1111/j.1600-065X.2009.00845.x>
- Pircher, T.J., J.N. Geiger, D. Zhang, C.P. Miller, P. Gaines, and D.M. Wojchowski. 2001. Integrative signaling by minimal erythropoietin receptor forms and c-Kit. *J. Biol. Chem.* 276:8995–9002. <http://dx.doi.org/10.1074/jbc.M007473200>
- Rhodes, M.M., P. Kopsombut, M.C. Bondurant, J.O. Price, and M.J. Koury. 2005. Bcl-x(L) prevents apoptosis of late-stage erythroblasts but does not mediate the antiapoptotic effect of erythropoietin. *Blood.* 106:1857–1863. <http://dx.doi.org/10.1182/blood-2004-11-4344>
- Rivella, S. 2012. The role of ineffective erythropoiesis in non-transfusion-dependent thalassemia. *Blood Rev.* 26:S12–S15. [http://dx.doi.org/10.1016/S0268-960X\(12\)70005-X](http://dx.doi.org/10.1016/S0268-960X(12)70005-X)
- Sathyanarayana, P., A. Dev, A. Pradeep, M. Ufkin, J.D. Licht, and D.M. Wojchowski. 2012. Spry1 as a novel regulator of erythropoiesis, EPO/EPOR target, and suppressor of JAK2. *Blood.* 119:5522–5531. <http://dx.doi.org/10.1182/blood-2011-11-392571>
- Singh, S., A. Dev, R. Verma, A. Pradeep, P. Sathyanarayana, J.M. Green, A. Narayanan, and D.M. Wojchowski. 2012a. Defining an EPOR-regulated transcriptome for primary progenitors, including Tnfr-sf13c as a novel mediator of EPO-dependent erythroblast formation. *PLoS ONE.* 7:e38530. <http://dx.doi.org/10.1371/journal.pone.0038530>
- Singh, S., R. Verma, A. Pradeep, K. Leu, R.B. Mortensen, P.R. Young, M. Oyasu, P.J. Schatz, J.M. Green, and D.M. Wojchowski. 2012b. Dynamic ligand modulation of EPO receptor pools, and dysregulation by polycythemia-associated EPOR alleles. *PLoS ONE.* 7:e29064. <http://dx.doi.org/10.1371/journal.pone.0029064>
- Stokes, M.P., C.L. Farnsworth, A. Moritz, J.C. Silva, X. Jia, K.A. Lee, A. Guo, R.D. Polakiewicz, and M.J. Comb. 2012. PTMScan direct: identification and quantification of peptides from critical signaling proteins by immunofluorescence enrichment coupled with LC-MS/MS. *Mol. Cell. Proteomics.* 11:187–201. <http://dx.doi.org/10.1074/mcp.M111.015883>
- Watowick, S.S. 2011. The erythropoietin receptor: molecular structure and hematopoietic signaling pathways. *J. Invest. Med.* 59:1067–1072.
- Welch, J.J., J.A. Watts, C.R. Vakoc, Y. Yao, H. Wang, R.C. Hardison, G.A. Blobel, L.A. Chodosh, and M.J. Weiss. 2004. Global regulation of erythroid gene expression by transcription factor GATA-1. *Blood.* 104:3136–3147. <http://dx.doi.org/10.1182/blood-2004-04-1603>
- Wojchowski, D.M., P. Sathyanarayana, and A. Dev. 2010. Erythropoietin receptor response circuits. *Curr. Opin. Hematol.* 17:169–176.
- Wu, H., X. Liu, R. Jaenisch, and H.F. Lodish. 1995. Generation of committed erythroid BFU-E and CFU-E progenitors does not require erythropoietin or the erythropoietin receptor. *Cell.* 83:59–67. [http://dx.doi.org/10.1016/0092-8674\(95\)90234-1](http://dx.doi.org/10.1016/0092-8674(95)90234-1)
- Zhang, J., and H.F. Lodish. 2007. Endogenous K-ras signaling in erythroid differentiation. *Cell Cycle.* 6:1970–1973. <http://dx.doi.org/10.4161/cc.6.16.4577>